IMPACT OF WETTING-DRYING CYCLES ON DYNAMIC TENSILE STRENGTH OF ROCK

by

Shengwei LI[a], Cunbao LI[b*], Wei YAO[a,c], Ru ZHANG[a], Jing XIE[a], Junchen ZHANG[c] Qiang LIU[a], and Zhaopeng ZHANG[a]

[a] State Key Laboratory of Hydraulics and Mountain River Engineering, College of Water Resource and Hydropower, Sichuan University, Chengdu, China
[b] Institute of Deep Earth Science and Green Energy, Shenzhen University, Shenzhen, China
[c] Department of Civil Engineering and Lassonde Institute, University of Toronto, Toronto, Canada

Original scientific paper
https://doi.org/10.2298/TSCI180411115L

To study the effect of wetting-drying cycles on dynamic tensile strength of rock, dynamic indirect tension test of sandstone samples after 0, 1, 3, and 5 wetting-drying cycles was conducted. Tensile failure was observed by digital image correlation. The result shows that failure appears in the center of the samples initially, consistent with tensile strain field results obtained by digital image correlation. An empirical formula was derived to link loading rate and dynamic tensile strength of rock after wetting-drying cycles. As the loading rate increases, tensile strength increases significantly. Tensile strength reduces as the number of wetting-drying cycles increases. These results provide reference data for complex engineering problems such as those that occur in coal mining, tunneling and water conservancy.

Key words: *sandstone, dynamic tensile strength, wetting-drying, Brazilian test, split Hopkinson pressure bar*

Introduction

Water influences the weakening of rocks in some geotechnical engineering applications, such as slope construction for dams, mining, and tunnel excavation, in which rock masses experience alternating dry and wet cycles caused by rain or river water levels rising and falling [1, 2]. In addition, dynamic loads caused by events such as earthquakes, blasting, and rock bursts result in many natural hazards. Therefore, the studies on dynamic mechanical properties of rock after wetting-drying (w-d) cycles are meaningful.

Recent studies have focused on the effect of w-d cycles on the effect of w-d cycles on the mechanical and physical properties of rocks. These studies have revealed that certain physical properties of density, weight, *etc.* decrease after cyclic wetting and drying, while porosity increases [3-7]. Mechanical properties including uniaxial compressive strength, tensile strength, and fracture toughness are also reduced after w-d cycles [8-14]. Hua *et al.* [8, 14, 15] analyzed the impact of w-d cycles on Mode I fracture toughness K_{IC} and Mode II fracture toughness K_{IIC} found that both K_{IIC}, and K_{IC} decrease as the number of cycles increases.

There is a significant difference between the dynamic and static mechanical behavior of rocks [16-18]. Only a few investigations have been conducted on dynamic mechanical properties of rock after w-d cycles. For instance, Yuan *et al.* [19] studied its effect on uniaxial

* Corresponding author, e-mail: cunbao.li@hotmail.com

compressive strength of rock under dynamic loading, and found that dynamic uniaxial compressive strength reduces when the number of cycles rises. Zhou *et al.* [2, 7] conducted dynamic compression and tension experiments on rocks and established a relationship between strain rate, the w-d cycle and the dynamic strength. Du *et al.* [20] conducted dynamic tensile test of red sandstone after w-d cycles and obtained the relationship between the fractal characteristics of rock fragmentation and the number of cycles.

However, there currently exists the contradiction the effect of w-d cycles on the dynamic and static mechanical behavior of rocks and the treatment methods and the number of cycles greatly affect the mechanical properties of rocks. Yuan *et al*. [19] found dynamic compression strength of sandstone is maximum after one w-d cycle, while Zhou *et al*. [2] found it increases with the number of w-d cycles using a different treatment method. In the research of Zhou *et al*. [2, 7], the numbers of cycles are 0, 10, 20, 30, 40, and 50; one cycle consists of samples placed into water for one day, and then air dried at 25 °C for at least six days. In the research of Du *et al*. [20], the numbers of cycles are 0, 5, 10, 15, and 20 and the samples are dried at 60 °C for 24 hours. In these experimental results, tensile strength changes fastest when the number of cycles changes from 0-10. Other researchers [8, 14, 15] adopted different treatment methods for w-d cycles, and the results of those experiments show that K_{IIC} and K_{IC} decrease as the numbers of cycles increase, for 0, 1, 3, 5, and 7 cycles. Thus, based on these treatment methods in [8, 14, 15], the dynamic tensile properties of rocks after 0, 1, 3, and 5 w-d cycles are studied in this work.

In this study, dynamic tensile tests of rock are carried out to study the influence of w-d cycles on dynamic tensile strength of sandstone. The digital image correlation (DIC) method was used to analyze tensile failure. The relationship between the loading rate and the tensile strength of sandstone after w-d cycles was obtained to provide a reference for complex engineering problems that arise in coal mining, tunneling, and water conservancy.

Sample preparation

Sandstone from Pingdingshan city, Henan Province, China, was used in this experiment. The main composition is quartz and feldspar. The density of the sandstone is 2.56 g/cm^3. The samples were made into discs recommended by the International Society for Rock Mechanics and Rock Engineering (ISRM) [21].

Based on previous research [8, 14, 15], sandstone samples were prepared after 0, 1, 3, and 5 w-d cycles. A w-d cycle included saturation and drying. First, to achieve saturation, the samples were placed in water for 24 hours. Second, an oven set at 105 °C was used to dry the saturated samples for one day. Finally, the dried samples were cooled to room temperature. After the cycles, the samples were placed in water for two days for testing. In this work, sandstone samples without w-d cycles were considered to have gone through 0 cycles.

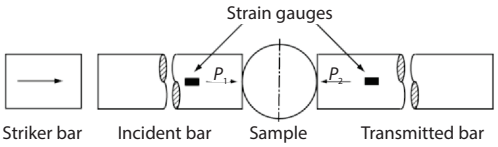

Figure 1. The schematic of the SHPB system

Experimental set-up

A 38-mm diameter split Hopkinson pressure bar (SHPB) system, as shown in fig. 1 was applied to carry out dynamic Brazilian disc (BD) experiments on the sandstone samples after 0, 1, 3, and 5 w-d cycles. The SHPB system, initially developed by Kolsky [22], has been recommended by the ISRM as a standard test facility [21]. It consists of three parts: striker, incident, and transmitted bar. After the incident waves enters the interface of the incident bar and specimen, some of them will be reflected back and the rest will pass through the sample and propagate through the transmitted bar.

Through the strains obtained from the stress waves, we can calculate the forces P_1 and P_2 on two sides of specimens using the following formula:

$$P_1 = EA\left(\varepsilon_i + \varepsilon_r\right) \tag{1}$$

$$P_2 = EA\varepsilon_t \tag{2}$$

where E and A are Young's modulus and the cross-sectional area of the bars, respectively, [23]. The ε_i, ε_r and ε_t are the incident, reflected and transmitted strains, respectively.

Based on the theory of elasticity, the tensile stress is:

$$\sigma(t) = \frac{2P(t)}{\pi DB} \tag{3}$$

where $P(t)$ is the diametrical load, D and B are diameter and thickness of the specimen, respectively. The maximum value of $\sigma(t)$ is dynamic tensile strength T_d.

Results and discussion

Dynamic force equilibrium and determination of loading rate

Dynamic force balance in the specimen is a precondition for dynamic testing. The pulse shaping technique was applied to achieve this equilibrium by using copper sheets [24-26]. According to eqs. (1) and (2), the dynamic forces, P_1, is proportional to the total of the incident (In) and reflected (Re) stress waves, and the dynamic forces, P_2, is proportional to transmitted (Tr) stress waves. As is shown in fig. 2, the dynamic forces P_1 and P_2 are nearly same during the dynamic loading period, indicating that dynamic force equilibrium is achieved.

The loading rate is determined through the time evolution of tensile stress in the middle of the BD sample. A typical tensile stress history is shown as fig. 3. There exists a region of approximately linear variation of stress with time from 125 to 175 μs in fig. 3. The slope of the linear phase was determined as loading rate [25]. Using this method, we can determine that the loading rate of the typical tensile stress history, $\dot{\sigma}$, is 190 GPa/s.

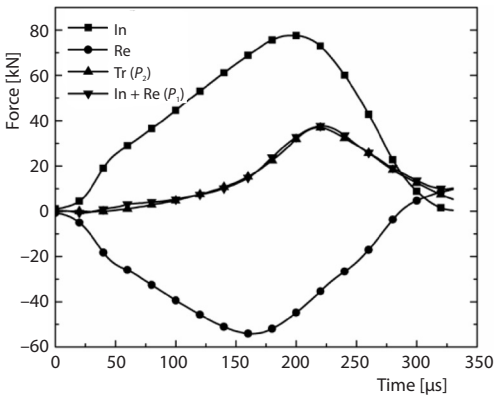

Figure 2. Dynamic force balance for a typical dynamic BD test

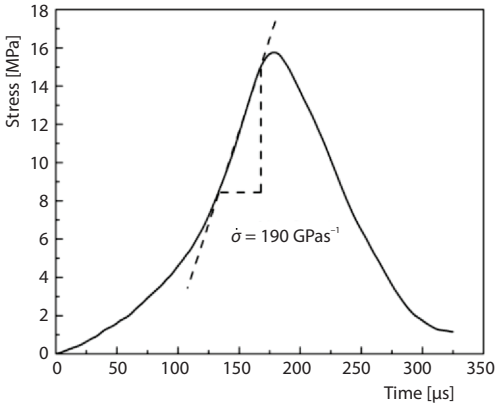

Figure 3. Typical tensile stress history

Tensile strength results

Figure 4 shows that the dynamic tensile strengths of samples, where N represents w-d cycles. It indicates that the tensile strengths of sandstone after different w-d cycles are

rate dependent. Besides, dynamic tensile strength is greatly influenced by w-d cycles. Strength reduces gradually as the number of cycles increases, which is consistent with static tensile strength results of Hua *et al.* [8]. After w-d cycles, internal micro-cracks in sandstone gradually increase as a result of the increase and decrease of water content, leading to the degradation of the dynamic tensile strength [2, 15].

Linear fitting curve are obtained to describe the variation of strength with loading rate. The fitted equations are given:

$$\left.\begin{aligned} T_d &= 0.0315\dot{\sigma} + 13.241,\ R^2 = 0.990 \quad (N=0)\\ T_d &= 0.0301\dot{\sigma} + 12.706,\ R^2 = 0.973 \quad (N=1)\\ T_d &= 0.0287\dot{\sigma} + 11.385,\ R^2 = 0.912 \quad (N=3)\\ T_d &= 0.0253\dot{\sigma} + 11.024,\ R^2 = 0.976 \quad (N=5) \end{aligned}\right\},\ (125 \le \dot{\sigma} \le 350) \tag{4}$$

where T_d is dynamic tensile strength, $\dot{\sigma}$ – the loading rate. Although the parameters in the equations for different cycles are different, the same form, $T_d = A\dot{\sigma} + B$ is used for all five w-d cycle conditions. Considering the relationship between A, B, and N, an empirical formula is proposed:

$$T_d = (0.0316 - 0.0012N)\dot{\sigma} - 0.4624N + 13.129,\ (125 \le \dot{\sigma} \le 350) \tag{5}$$

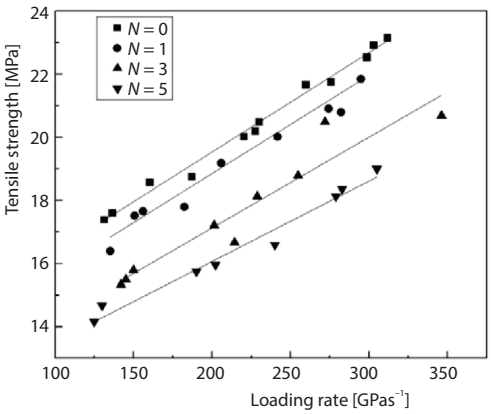

Figure 4. Tensile strength results for sandstone after cyclic wetting and drying

As shown in fig. 4, this empirical formula matches the data trend well.

Using DIC with a high-speed camera to record tensile failure

The DIC technique has been widely used for non-contact deformation measurements [27]. In this work, a high-speed camera was used to investigate fracture processes during dynamic tensile testing. The DIC technique was applied to analyze stress and strain of samples. The dynamic split failure process and the tensile strain distribution of sandstone specimens are presented in fig. 5.

Figure 5 shows that tensile failure occurs initially at the center of the specimen, and expands to both sides of the specimen along the loading direction until the specimen undergo a split failure. This indicates that the dynamic split tests satisfy the assumption of Griffith strength. The results are also consistent with those results reported by other researchers [17, 28-30].

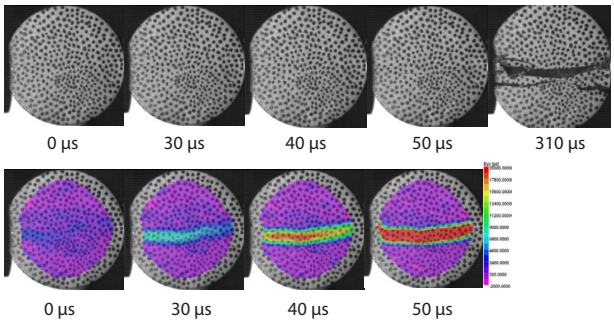

Figure 5. Dynamic split failure process of sandstone samples and tensile strain distribution

From the tensile strain distributions obtained by the DIC analysis, it is observed that the tensile strain extends from the area near the incident bar to the area near the transmitted

bar. The maximum tensile strain occurs in the center of the disc, which proves that the validity of the dynamic indirect tensile test.

Conclusion

In this work, we studied the influence of w-d cycles on dynamic tensile strength of rock. After 0, 1, 3, and 5 w-d cycles the sandstone specimens underwent dynamic tensile loading using the SHPB system and the BD method. Tensile failure was observed by the DIC method.

The tensile failure appears initially in the center of the BD samples, which is consistent with the tensile strain field obtained by the DIC. As loading rate increases, tensile strength increases significantly. The cyclic treatments degrade the dynamic properties of sandstone. An empirical formula links the loading rate and the tensile strength during w-d cycles. The results provide reference data for complex engineering problems that occur in coal mining, tunneling, and water conservancy.

Acknowledgment

This work was financially supported by National Natural Science Foundation of China (Grant No. 51822403, Grant No. 51622402, Grant No. 51674170), State Key Laboratory of Hydraulics and Mountain River Engineering (SKHL) (Grant No. SKHL1606) and The Fundamental Research Funds for the Central Universities (Grant No. 2012017yjsy168).

Nomenclature

A – cross-sectional area of the bars, [mm^2]
B – the thickness of the BD specimen, [mm]
D – diameter of the BD specimen, [mm]
E – Young's modulus of the bars, [GPa]
N – the number of wetting and drying cycles, [–]
P_1 – force on the incident end of the BD specimen, [kN]
P_2 – force on the transmitted end of the BD specimen, [kN]
$P(t)$ – time-varying load recorded in the test, [kN]
T_d – dynamic tensile strength, [MPa]

Greek symbols

ε_i – incident strain, [–]
ε_r – reflected strain, [–]
ε_t – transmitted strain, [–]
$\sigma(t)$ – tensile stress at the center of the BD specimen, [MPa]
$\dot{\sigma}$ – loading rate, [GPa/s]

References

[1] Xie, H., *et al.*, Research and Development of Rock Mechanics in Deep Ground Engineering (in Chinese), *Chinese Journal of Rock Mechanics and Engineering*, *34* (2015), 11, pp. 2161-2178
[2] Zhou, Z., *et al.*, Influence of Cyclic Wetting and Drying on Physical and Dynamic Compressive Properties of Sandstone, *Engineering Geology*, *220* (2017), Mar., pp. 1-12
[3] Kassab, M. A., *et al.*, Study on P-Wave and S-Wave Velocity in Dry and Wet Sandstones of Tushka Region, Egypt, *Egyptian Journal of Petroleum*, *24* (2015), 1, pp. 1-11
[4] Ozbek, A., Investigation of the Effects of Wetting-Drying and Freezing-Thawing Cycles on Some Physical and Mechanical Properties of Selected Ignimbrites, *Bulletin of Engineering Geology and the Environment*, *73* (2013), 2, pp. 595-609
[5] Sumner, P. D., *et al.*, Experimental Sandstone Weathering Using Different Wetting and Drying Moisture Amplitudes, *Earth Surface Processes and Landforms*, *33* (2008), 6, pp. 985-990
[6] Pardini, G., *et al.*, Structure and Porosity of Smectitic Mudrocks as Affected by Experimental Wetting-Drying Cycles and Freezing-Thawing Cycles, *Catena*, *27* (1996), 27, pp. 149-165
[7] Zhou, Z., *et al.*, Dynamic Tensile Properties of Sandstone Subjected to Wetting and Drying Cycles, *Construction and Building Materials*, *182* (2018), Sept., pp. 215-232
[8] Hua, W., *et al.*, The Influence of Cyclic Wetting and Drying on the Fracture Toughness of Sandstone, *International Journal of Rock Mechanics and Mining Sciences*, *78* (2015), June, pp. 331-335
[9] Liu, X., *et al.*, Macro/Microtesting and Damage and Degradation of Sandstones under Dry-Wet Cycles, *Advances in Materials Science and Engineering*, *2016* (2016), Mar., pp. 1-16

[10] Yuan, W., *et al.*, Study on Deterioration of Strength Parameters of Sandstone under the Action of Dry-Wet Cycles in Acid and Alkaline Environment, *Arabian Journal for Science and Engineering*, *43* (2018), 1, pp. 335-348
[11] Zhang, B., *et al.*, Deformation and Shear Strength of Rockfill Materials Composed of Soft Siltstones Subjected to Stress, Cyclical Drying/Wetting and Temperature Variations, *Engineering Geology*, *190* (2015), May, pp. 87-97
[12] Zhao, Z., *et al.*, Effects of Wetting and Cyclic Wetting-Drying on Tensile Strength of Sandstone with a Low Clay Mineral Content, *Rock Mechanics and Rock Engineering*, *50* (2016), 2, pp. 485-491
[13] Hale, P. A., A Laboratory Investigation of the Effects of Cyclic Heating and Cooling, Wetting and Drying, and Freezing and Thawing on the Compressive Strength of Selected Sandstones, *Environmental and Engineering Geoscience*, *9* (2003), 2, pp. 117-130
[14] Hua, W., *et al.*, Experimental Investigation on the Effect of Wetting-Drying Cycles on Mixed Mode Fracture Toughness of Sandstone, *International Journal of Rock Mechanics and Mining Sciences*, *93* (2017), Mar., pp. 242-249
[15] Hua, W., *et al.*, Effect of Cyclic Wetting and Drying on the Pure Mode Ii Fracture Toughness of Sandstone, *Engineering Fracture Mechanics*, *153* (2016), Mar., pp. 143-150
[16] Xia, K., *et al.*, Dynamic Rock Tests Using Split Hopkinson (Kolsky) Bar System – A Review, *Journal of Rock Mechanics and Geotechnical Engineering*, *7* (2015), 1, pp. 27-59
[17] Zhang, Q., *et al.*, A Review of Dynamic Experimental Techniques and Mechanical Behaviour of Rock Materials, *Rock Mechanics and Rock Engineering*, *47* (2013), 4, pp. 1411-1478
[18] Gao, M., *et al.*, Field Experiments on Fracture Evolution and Correlations between Connectivity and Abutment Pressure under Top Coal Caving Conditions, *International Journal of Rock Mechanics and Mining Sciences*, *111* (2018), Nov., pp. 84-93
[19] Yuan, P., *et al.*, Split Hopkinson Pressure Bar Test on Sandstone in Coalmine under Cyclic Wetting and Drying (in Chinese), *Rock and Soil Mechanics*, *34* (2013), 9, pp. 2557-2562
[20] Du, B., *et al.*, Experimental Study on the Dynamic Tensile Mechanical Properties of Red-Sandstone after Cyclic Wetting and Drying (in Chinese), *Chinese Journal of Rock Mechanics and Engineering*, *37* (2018), Apr., pp. 1-7
[21] Zhou, Y., *et al.*, Suggested Methods for Determining the Dynamic Strength Parameters and Mode-I Fracture Toughness of Rock Materials, *International Journal of Rock Mechanics and Mining Sciences*, *49* (2012), Jan., pp. 105-112
[22] Kolsky, H., An Investigation of the Mechanical Properties of Materials at Very High Rates of Loading, *Proceedings of the physical society, Section B*, *62* (1949), 11, pp. 676-700
[23] Yao, W., *et al.*, Dependence of Dynamic Tensile Strength of Longyou Sandstone on Heat-Treatment Temperature and Loading Rate, *Rock Mechanics and Rock Engineering*, *49* (2016), 10, pp. 3899-3915
[24] Frew, D., *et al.*, Pulse Shaping Techniques for Testing Brittle Materials with a Split Hopkinson Pressure Bar, *Experimental Mechanics*, *42* (2002), 1, pp. 93-106
[25] Dai, F., *et al.*, A Semi-Circular Bend Technique for Determining Dynamic Fracture Toughness, *Experimental Mechanics*, *50* (2010), 6, pp. 783-791
[26] Yao, W., *et al.*, Dynamic Mechanical Behaviors of Fangshan Marble, *Journal of Rock Mechanics and Geotechnical Engineering*, *9* (2017), 5, pp. 807-817
[27] Chen, Z., *et al.*, Optimized Digital Speckle Patterns for Digital Image Correlation by Consideration of Both Accuracy and Efficiency, *Applied optics*, *57* (2018), 4, pp. 884-893
[28] Zhang, Q., *et al.*, Determination of Mechanical Properties and Full-Field Strain Measurements of Rock Material under Dynamic Loads, *International Journal of Rock Mechanics and Mining Sciences*, *60* (2013), Mar., pp. 423-439
[29] Yin, T., *et al.*, Effects of Thermal Treatment on Tensile Strength of Laurentian Granite Using Brazilian Test, *Rock Mechanics and Rock Engineering*, *48* (2015), 6, pp. 2213-2223
[30] Chen, R., *et al.*, Flattened Brazilian Disc Method for Determining the Dynamic Tensile Stress-Strain Curve of Low Strength Brittle Solids, *Experimental Mechanics*, *53* (2013), 7, pp. 1153-1159

Paper submitted: April 11, 2018
Paper revised: July 10, 2018
Paper accepted: October 10, 2018